PERGAMON

International Journal of Heat and Mass Transfer 44 (2001) 2193–2197

International Journal of HEAT and MASS TRANSFER

www.elsevier.com/locate/ijhmt

Technical Note

Initial transient behavior during close-contact melting induced by convective heating

Hoseon Yoo *

Department of Mechanical Engineering, Soongsil University, Seoul 156-743, South Korea

Received 4 February 2000; received in revised form 14 June 2000

1. Introduction

Close-contact melting has attracted considerable research interests mainly due to high heat transfer rate and/or low friction between two solid bodies concerned. Its basic principle, research results, and applications can be found in a recent review [1]. Focusing our attention on simplifications associated with theoretical modeling, most of the previous works have relied on the assumption of quasi-steady processes. In order to justify the assumption or to better understand the unsteady behavior involved there, time-dependent approaches are needed. Such attempts, however, have been made only in a few studies [2,3].

Lately, an analysis for the transient close-contact melting occurring on a flat surface has been reported [4], in which a pair of analytical solutions for constant wall temperature and constant heat flux conditions were derived. In connection with thermal boundary conditions, it is known that in thermally developed duct flows, convective heat transfer from an isothermal external fluid to the duct surface includes both uniform wall temperature and uniform heat flux conditions as limiting cases [5]. This aspect seems to be applicable to close-contact melting by adequately replacing the axial variation of the wall heat flux with its time evolution, though the two situations are different from each other.

This work is aimed at analyzing the initial transient process from the beginning to the steady state of close-contact melting induced by convective heating. The previous study [4] is extended to obtain an analytical solution for a more general thermal condition. Emphasis is placed on the reduction procedure to make model equations cover both constant heat flux and constant wall temperature limits.

2. Modeling

The physical system considered in this work is depicted in Fig. 1. A solid block at its fusion temperature T_m melts on a flat plate that is convectively heated by an isothermal fluid at T_∞ ($> T_m$). As the melting proceeds at the solid–liquid interface, a thin liquid film is formed between the solid and plate and grows with time. Simultaneously with the film growth, the solid block moves downward by its own weight. This motion leads the liquid generated by melting to flow outward, being squeezed out along the periphery. Both the liquid film thickness δ and the solid descending velocity V keep varying toward the steady state when they are invariant.

The convective heat transfer between the fluid and plate can be described in a similar manner to that in thermally developed duct flows [6]. Assuming the plate thickness and its thermal resistance are negligible, the instantaneous heat flux can be expressed as

$$q'' = h_e[T_\infty - T_w(t)], \tag{1}$$

where h_e is presumed to be constant. Two limiting cases of convective heating are distinguished by the Biot number that is defined as the ratio of external to internal conductances, i.e., $Bi = h_e R/k$, where R is a characteristic length. Since R is also related to nondimensionalization of other quantities, its choice is problem-dependent. When Bi is large, the wall temperature approaches the isothermal condition, $T_w = T_\infty$. When Bi is small, q'' can be treated as constant because the wall temperature is so throttled by the external resistance (h_e^{-1}) as to vary quite slowly with time.

* Tel.: +82-2-820-0661; fax: +82-2-814-3627.
E-mail address: hsyoo@engineer.ssu.ac.kr (H. Yoo).

PII: S0017-9310(00)00233-7

Nomenclature

B	coefficient, $Bi\ \widetilde{\delta}_c$
Bi	Biot number, $h_e R/k$
c	liquid specific heat
F	consolidated parameter, $\widetilde{g}\widetilde{H}/(GPr)$
g	gravitational acceleration, Fig. 1
$\widetilde{g}$	dimensionless gravitational acceleration, gR^3/α^2
G	geometrical parameter of solid block
h_e	heat transfer coefficient, Fig. 1
h_{sf}	latent heat of fusion
H	height of solid block, Fig. 1
$\widetilde{H}$	dimensionless solid height, H/R
k	liquid thermal conductivity
M	mass of solid block, Fig. 1
Nu	Nusselt number, Eq. (15)
$\widehat{Nu}$	normalized Nusselt number, Eq. (16)
$\langle\widehat{Nu}\rangle$	mean normalized Nusselt number, Eq. (18)
P	pressure in the liquid film
Pr	Prandtl number, $\mu c/k$
q''	supplied heat flux, Eq. (1)
R	characteristic length
S	contact area
Ste	Stefan number, $c(T_\infty - T_m)/h_{sf}$
t	time
$\widetilde{t}$	dimensionless time, $t\alpha/R^2$
$\widehat{t}$	normalized time, $\widetilde{t}\widetilde{V}_c/(\widetilde{\rho}\widetilde{\delta}_c)$
$\widehat{t}_u$	normalized transient period
T	temperature
T_∞	heating fluid temperature, Fig. 1
T_m	fusion temperature of the solid, Fig. 1
T_w	heating wall temperature, Fig. 1
$\widehat{T}_w$	normalized wall temperature, Eq. (17)
V	solid descending velocity, Fig. 1
$\widetilde{V}$	dimensionless solid descending velocity, VR/α
$\widehat{V}$	normalized solid descending velocity, $\widetilde{V}/\widetilde{V}_c$
z	vertical coordinate, Fig. 1

Greek symbols

α	liquid thermal diffusivity, $k/(\rho_l c)$
δ	liquid film thickness, Fig. 1
$\widetilde{\delta}$	dimensionless liquid film thickness, δ/R
$\widehat{\delta}$	normalized liquid film thickness, $\widetilde{\delta}/\widetilde{\delta}_c$
ρ	density
$\widetilde{\rho}$	density ratio, ρ_l/ρ_s

Subscripts

c	steady state
l	liquid phase
s	solid phase

In order to render the problem analytically tractable, some assumptions that have been commonly adopted in close-contact melting analyses [4,7–9] are introduced. The thin film approximation is invoked, so that the z-directional conduction dominates heat transport. In addition, a decrease in the solid mass during the transient process is neglected.

The transient behavior can be represented by time evolution of δ and V, for which two equations are needed. One is the force balance between the pressure in the liquid film and the weight and inertia of the descending solid

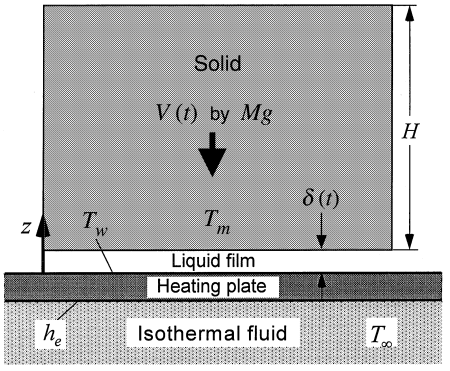

Fig. 1. Schematic of the present close-contact melting system.

$$M\left(g - \frac{\mathrm{d}V}{\mathrm{d}t}\right) = \int_s P\,\mathrm{d}S. \tag{2}$$

The inertia term is neglected additionally because the acceleration of descending motion is much smaller than that of gravity. The other is the energy conservation at the melting front

$$-k\left.\frac{\partial T}{\partial z}\right|_{z=\delta} = \rho_s h_{sf}\left(V + \frac{\mathrm{d}\delta}{\mathrm{d}t}\right). \tag{3}$$

3. Analysis

For the closure of modeling, the pressure force and interfacial temperature gradient involved in the above model equations should be expressed in terms of dependent variables. This can be done by solving the continuity, momentum, and energy equations in the liquid film.

Since the thermal condition at issue is irrelevant directly to the force balance, the already established pressure distribution [4,7,9] can be applied to Eq. (2). Without repeating the detailed procedure, the result cast in a dimensionless form is cited here.

$$\widetilde{V} + (1-\widetilde{\rho})\frac{\mathrm{d}\widetilde{\delta}}{\mathrm{d}\widetilde{t}} = \left(\frac{\widetilde{g}\widetilde{H}}{GPr}\right)\widetilde{\delta}^3, \tag{4}$$

where dimensionless quantities are defined in Nomenclature. The parameter G represents the geometric configuration of the solid block, and its value depends on the characteristic length used in each analysis. When the solid is two-dimensionally rectangular or circularly cylindrical with a half of the width or the radius as the length scale, G is a constant [7]. When the solid is a rectangular parallelepiped with a square root of cross-sectional area as the length scale, G is expressed as a function of the aspect ratio of a contact surface [4].

Due to the thin film approximation, the energy equation results in a linear temperature profile across the liquid layer, which leads Eq. (3) to

$$\frac{k(T_w - T_m)}{\delta} = \rho_s h_{sf}\left(V + \frac{d\delta}{dt}\right). \tag{5}$$

After the unknown T_w is replaced by T_∞ using Eq. (1), it is nondimensionalized as

$$\widetilde{V} + \frac{d\widetilde{\delta}}{d\widetilde{t}} = \widetilde{\rho} Ste \frac{Bi}{1 + Bi\,\widetilde{\delta}}. \tag{6}$$

While Eq. (6) properly reflects the isothermal limit at a large extreme of Bi, it merely shows no melting at its small extreme. That is, it fails to meet our aim that the model equations include both constant heat flux and constant wall temperature conditions as limiting cases. This problem may be overcome by further reducing the model equations. In view of the previous study [4], a way is normalization based on the steady solution.

Since the time derivatives vanish at the steady state, the steady solution is readily obtained. Rearranging Eqs. (4) and (6) leads to

$$\widetilde{\delta}_c^3 + Bi\,\widetilde{\delta}_c^4 = \widetilde{\rho} Ste\, Bi F^{-1}, \quad \widetilde{V}_c = F\widetilde{\delta}_c^3. \tag{7}$$

For a small Bi, noting that $\widetilde{\delta}_c \ll 1$ under a normal close-contact melting condition, the second term on the left-hand side of Eq. (7) can be neglected to yield

$$\widetilde{\delta}_c = (\widetilde{\rho} Ste)^{1/3} F^{-1/3} Bi^{1/3}, \quad \widetilde{V}_c = (\widetilde{\rho} Ste)\, Bi. \tag{8}$$

For a large Bi, the solution is derived as

$$\widetilde{\delta}_c = (\widetilde{\rho} Ste)^{1/4} F^{-1/4}, \quad \widetilde{V}_c = (\widetilde{\rho} Ste)^{3/4} F^{1/4}. \tag{9}$$

It is confirmed that the results for two limiting cases coincide with the known steady solutions for constant heat flux and constant wall temperature conditions, respectively [4].

Using definitions in Nomenclature, along with the steady solution (7), Eqs. (4) and (6) are normalized, respectively, as

$$\widehat{V} + \frac{(1 - \widetilde{\rho})}{\widetilde{\rho}} \frac{d\widehat{\delta}}{d\widehat{t}} = \widehat{\delta}^3, \tag{10}$$

$$\widehat{V} + \frac{1}{\widetilde{\rho}} \frac{d\widehat{\delta}}{d\widehat{t}} = \frac{1 + B}{1 + B\widehat{\delta}}. \tag{11}$$

Eq. (11) differs from Eq. (6) in that its right-hand side approaches the constant heat flux limit, i.e., 1, as B (or Bi) reaches the smallest extreme. Now, the model equations set up for convective heating include both of the limiting cases.

The solution procedure is straightforward. Subtracting Eq. (10) from (11), we have

$$\frac{d\widehat{\delta}}{d\widehat{t}} = \frac{1 + B}{1 + B\widehat{\delta}} - \widehat{\delta}^3. \tag{12}$$

This is integrated to give

$$\widehat{t} = \int_0^{\widehat{\delta}} \left(\frac{1 + B}{1 + B\zeta} - \zeta^3\right)^{-1} d\zeta, \tag{13}$$

where the initial condition $\widehat{\delta}(0) = 0$ has been applied. The $\widehat{\delta} - \widehat{t}$ relation can be evaluated through a numerical integration. Once $\widehat{\delta}(\widehat{t})$ is known, $\widehat{V}(\widehat{t})$ is determined from

$$\widehat{V} = \frac{(\widetilde{\rho} - 1)}{\widetilde{\rho}} \frac{1 + B}{1 + B\widehat{\delta}} + \frac{\widehat{\delta}}{\widetilde{\rho}}. \tag{14}$$

Eq. (13) admits analytical integrations for the two limiting cases, the results of which are identical with the previous solutions that were derived separately [4].

The heat transfer rate between the fluid and system is characterized by the Nusselt number defined as [6]

$$Nu = \frac{q''}{T_\infty - T_m} \frac{R}{k}. \tag{15}$$

This can be rewritten as $Nu = Bi/(1 + B\widehat{\delta})$. For the same reason as in Eq. (6), the normalized Nusselt number is used here

$$\widehat{Nu} = (1 + B)/(1 + B\widehat{\delta}). \tag{16}$$

The wall temperature is another variable of interest since it is easier to measure than the others, e.g., δ and V. Its normalized form is

$$\widehat{T}_w = \frac{T_w - T_m}{T_{wc} - T_m} = \frac{(1 + B)\widehat{\delta}}{1 + B\widehat{\delta}}. \tag{17}$$

As Bi approaches the limiting values, Eq. (17) reduces to $\widehat{T}_w = \widehat{\delta}$ and 1, respectively.

4. Results and discussion

It has been repeatedly shown that two limiting cases of convective heating correspond to constant heat flux and constant wall temperature conditions, respectively. This means that the present work includes the previous

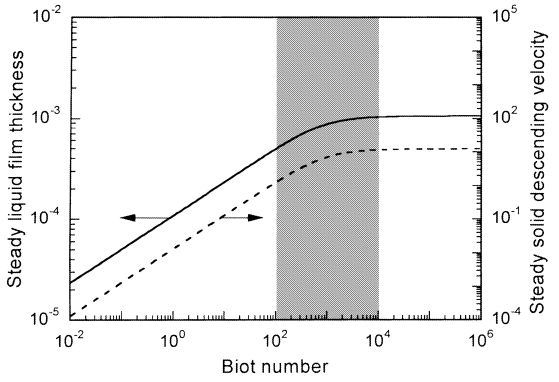

Fig. 2. Dependence of steady solution on Biot number.

study [4] as a subset. The present analysis can be justified by the already validated limiting cases.

Among various parameters, the focus here is on the Biot number. In the calculations presented below, all the other conditions have been fixed at typical values [2]: $\widetilde{g} = 5.521 \times 10^{11}, \widetilde{\rho} = 1.0, \widetilde{H} = 1.0, G = 4.0, Pr = 13.44$, and $Ste = 0.01266$, hence $F = 1.027 \times 10^{10}$.

The dependence of steady liquid film thickness $\widetilde{\delta}_c$ and solid descending velocity $\widetilde{V}_c$ on Bi is delineated in Fig. 2. In view of the variation patterns, close-contact melting induced by convective heating can be divided into three regimes, viz., constant heat flux, intermediate (shaded in the plot), and isothermal. This work is the first to deal with the intermediate regime. Depending on the conditions other than Bi, the bounds of each regime turn out to shift, but the basic pattern remains unchanged. The curves in the constant heat flux and isothermal regimes agree with the limiting solutions (7) and (8), respectively.

Five values of Bi are selected to show the effect of supplied heat flux on the initial transient behavior. Two of them are small and large extremes of Bi, and the rest belong to the intermediate regime: $Bi = 300$, 1000, and 3000. Fig. 3 shows time evolution of the normalized liquid film thickness $\widehat{\delta}$ and solid descending velocity $\widehat{V}$. In these plots, two curves for the limiting cases form the lower and upper bounds of evolution paths. Three intermediate ones lie inside the envelope without intersecting. As Bi increases, they gradually shift from the lower to upper bounds, showing a similar trend.

Eq. (17) can be used for predicting the transient behavior by monitoring the wall temperature variation in experiments. Fig. 4 illustrates time evolution of the normalized wall temperature $\widehat{T}_w$ for the five values of Bi. The curve for the smallest Bi seems to vary sharply in the normalized time scale. However, the heat flux remains nearly constant because the transient period (i.e., the duration from the beginning to the steady state of melting) in real time is long. Note that the time scale is of the order of $Bi^{-2/3}$ in Eq. (8). Since Bi is the only parameter involved in this plot, the heat transfer coefficient h_e in an experiment can be evaluated simply by selecting a calculated $\widehat{T}_w(\widehat{t})$ curve that fits best the measured variation of the wall temperature.

The normalized Nusselt number needs no further explanation since it is self-evident in Eq. (16) and Fig. 3(a). Instead, heat transfer characteristics during the transient process can better be shown by the mean normalized Nusselt number defined as

$$\langle \widehat{Nu} \rangle = \frac{1}{\widehat{t}_u} \int_0^{\widehat{t}_u} \widehat{Nu}\, d\widehat{t}. \tag{18}$$

Although the value of $\widehat{t}_u$ depends on its definition [4], $\widehat{t}_u = 2.0$, which is roughly estimated from Fig. 3, is used here. Fig. 5 elucidates the dependence of $\langle \widehat{Nu} \rangle$ on Bi. The curve asymptotically approaches the limiting values as

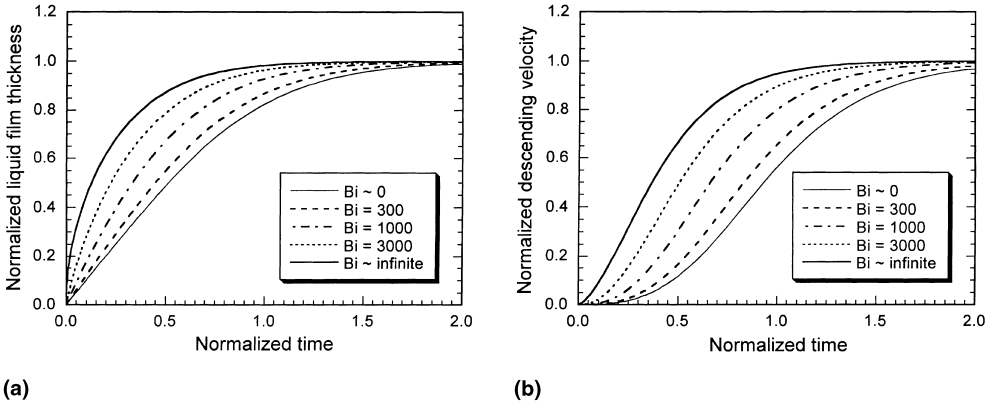

Fig. 3. Time evolution of normalized dependent variables for five Biot numbers: (a) liquid film thickness; (b) solid descending velocity.

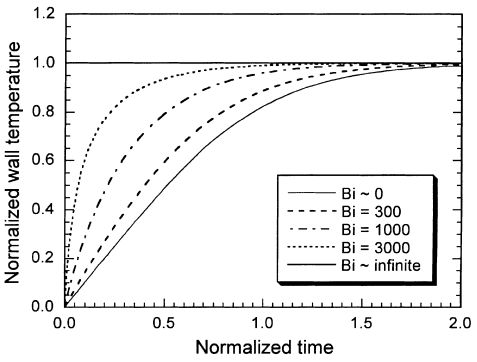

Fig. 4. Time evolution of normalized wall temperature for five Biot numbers.

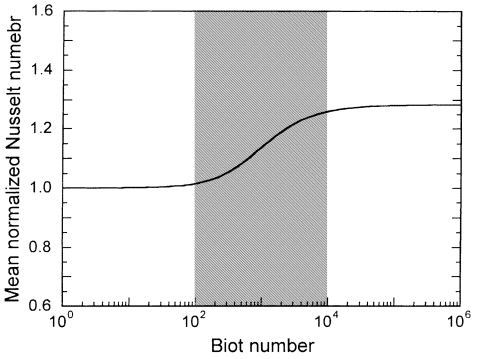

Fig. 5. Dependence of mean normalized Nusselt number on Biot number.

Bi reaches small and large extremes, while varying sharply in the intermediate regime, which is similar to that for thermally developed duct flows [6]. The limiting value of $\langle \widehat{Nu} \rangle$ for the smallest *Bi* is unity, and that for the other extreme is obtained, via some mathematical manipulations, as

$$\langle \widehat{Nu} \rangle = \frac{1}{\widehat{t}_u} \int_0^{\widehat{t}_u} \coth^{1/2}(2\widehat{t})\, \mathrm{d}t = \frac{1}{2}\left(1 + \frac{\pi}{\widehat{t}_u}\right). \tag{19}$$

Note that both of the two limiting values of $\langle \widehat{Nu} \rangle$ are constant.

5. Conclusions

This work has investigated the initial transient behavior during close-contact melting on a flat plate that is convectively heated by an isothermal fluid. Using normalization based on the steady solution, the model equations set up for convective heating have been modified to include both constant heat flux and constant wall temperature conditions as limiting cases. In this procedure, the properties of steady solution have also been clarified. The normalized model equations yield a compactly expressed analytical solution.

Depending on the Biot number, close-contact melting induced by convective heating can be divided into three regimes: constant heat flux, intermediate, and isothermal. The constant heat flux and isothermal limits serve as the lower and upper bounds on time evolution of the normalized variables. Finally, the mean normalized Nusselt number is proved to vary monotonically between the two limiting values, which is similar to the established fact in thermally developed duct flows.

References

[1] A. Bejan, Contact melting heat transfer and lubrication, Adv. Heat Transfer 24 (1994) 1–38.
[2] H. Hong, A. Saito, Numerical method for direct contact melting in transient process, Int. J. Heat Mass Transfer 36 (1993) 2093–2103.
[3] A. Saito, H. Kumano, S. Okawa, K. Yamashita, Analytical study on transient direct contact melting phenomena, Trans. Jpn. Assoc. Refrigeration 13 (1996) 97–108.
[4] H. Yoo, Analytical solutions to the unsteady close-contact melting on a flat plate, Int. J. Heat Mass Transfer 43 (2000) 1457–1467.
[5] E.M. Sparrow, S.V. Patankar, Relationship among boundary conditions and Nusselt numbers for thermally developed duct flows, J. Heat Transfer 99 (1977) 483–485.
[6] A. Bejan, Convection Heat Transfer, second ed., Wiley, New York, 1995, pp. 118–121.
[7] M.K. Moallemi, B.W. Webb, R. Viskanta, An experimental and analytical study of close-contact melting, J. Heat Transfer 108 (1986) 84–899.
[8] K. Taghavi, Analysis of direct-contact melting under rotation, J. Heat Transfer 112 (1990) 137–143.
[9] A. Bejan, The fundamentals of sliding contact melting and friction, J. Heat Transfer 111 (1989) 13–20.